

Core to Solar Wind: A Stepwise Model for Heating the Solar Corona

Claudio Vita-Finzi *

Earth Sciences, Natural History Museum, Cromwell Road, London SW7 5BD, UK

* **Corresponding author:** Claudio Vita-Finzi. Earth Sciences, Natural History Museum, Cromwell Road, London SW7 5BD, UK, E-mail: cvitafinzi@aol.com

Received date: 13-September-2022, Manuscript No. tspa-22-74433; **Editor assigned:** 15-September-2022, PreQC No. tspa-22-74433 (PQ);

Reviewed: 23-September-2022, QC No. tspa-22-74433 (Q); **Revised:** 24-September-2022, Manuscript No. tspa-22-74433 (R); **Published:** 30-September-2022, DOI No. 10.37532/2320-6756.2022.10(9).297

Abstract

The model outlined here embodies three distinct, successive processes which both define and characterize the Sun's chromosphere, transition region and corona. Operating experience from fusion research shows how Spitzer resistivity may render ohmic heating in the chromosphere self-limiting and thus serve to define the lower margin of the transition region; its upper margin is at $\sim 6.10^3$ K, where radiative cooling of He/H plasma decelerates sharply. The third and last stage in the proposed scheme is expansion into the tenuous plasma of space, which leads to the acceleration of ions to high energies, long recorded by spacecraft instruments as He^{++} . There is thus dynamic continuity all the way from the solar interior - the energy source for spinning columns in the Rayleigh-Bénard setting of the convection zone - to the coronal exhalation of the solar wind, a finding which should benefit the analysis of space weather, witness the association between helium in the solar wind and the incidence of coronal mass ejections.

Keywords: Sun; Photosphere; Chromosphere; Transition region; Corona

Introduction

The high temperature (≥ 1 to 2.10^6 K) of the Sun's outermost atmosphere or corona was identified in 1939 but has still to be explained. The mechanisms currently most in favour emphasize magnetic reconnection or waves of some kind and they treat the chromosphere and corona together [1]. This paper develops an alternative scheme which links the Sun's interior with its atmosphere in three stages corresponding to (and indeed identifying) the photosphere-chromosphere, the transition region and the corona [2].

Bearing in mind that any analogy between processes on the Sun and in terrestrial laboratories particularly fusion is only approximate, there are instructive parallels between the first step in our model and the early stages of a conventional tokamak operation especially as laboratory experiments for these conditions are not available [3]. There a toroidal current serves the dual purpose of confining the plasma and heating it. As the main contours of the solar body represent the interplay between gravitational contraction and thermal expansion, the solar environment performs confinement effectively though imperfectly, thus freeing the available magnetic energy from this task. In fact, as indicated by the solar wind, there is a net surplus of plasma to sustain the chromosphere.

Citation: Vita-Finzi C, Core to Solar Wind: A Stepwise Model for Heating the Solar Corona. J. Phys. Astron. 2022;10(9):297.

©2022 Trade Science Inc.

Step 1

Plasma composition as well as induction heating shows qualified kinship between Sun and laboratory, although in a tokamak the favoured fuel deuterium-tritium is fully ionized at the temperatures required for fusion ($\sim 10^8$ K). The H:He ratio may dominate discussion of the influence of elemental abundance on chromospheric heating, with a photospheric bulk composition of H 90.965% and He 8.89%. Sodium, magnesium, calcium, and iron are also present, a fact that is exploited in particular in the assessment of fractionation between the photosphere and different varieties of solar wind [4]. The impurities that have been detected during the ohmic heating phase of JET operation, such as reactor wall material (Ni, Cr, Fe), oxygen, carbon, molybdenum and chlorine, lead to radiation losses and presumably do so in the solar reactor [5].

The accepted view is that the temperature of the chromosphere rises from $66 \cdot 10^2$ K at its contact with the photosphere to $\sim 3 \cdot 10^4$ K over a distance of $\sim 25 \cdot 10^5$ m [6]. In our proposed tripartite scheme the weakly ionized H α of the chromosphere is subject to ohmic (or Joule) heating. In accordance with the account by Spitzer the resistance and thus the efficacy of ohmic heating decrease in proportion to the electron temperature as $T_e^{-3/2}$, so that there is a point at which ohmic heating stalls [7]. Owing to operational constraints ohmic heating at startup in most tokamaks can attain at most ~ 1 keV, say 10^7 K, as is the case with the JET tokamak [8,9].

It has been suggested that the temperature of the chromosphere ‘steadfastly refuses to rise above 10^4 K until hydrogen becomes fully ionized’ perhaps because ‘ionization of hydrogen leads to a high specific heat’ [10]. The issue of specific heat had previously been raised in a study of the Jovian atmosphere for which an atmospheric composition of hydrogen and helium was postulated [11]. A non-dimensional plot of specific heat against temperature at $1 - 6 \cdot 10^4$ K for particle densities from 10^{10} g cm^{-3} to 10^{-6} g cm^{-3} and for hydrogen unit volumes of 0.333 and 1.0 (equivalent to 50% and 100% hydrogen by volume) yields two prominent peaks **FIG. 1**. The greater is at 2.5 to $4 \cdot 10^4$ K, which may be manifested as a heightened but short-lived response to ohmic heating when the transiting gas attains a critical temperature. This specific heat imposes an upper limit on the chromospheric temperature well below the Spitzer limit. Indeed, the temperature in the Sun, after a temporary reversal, increases only to $\sim 2 \cdot 10^4$ K some $3 \cdot 10^3$ km above the photosphere.

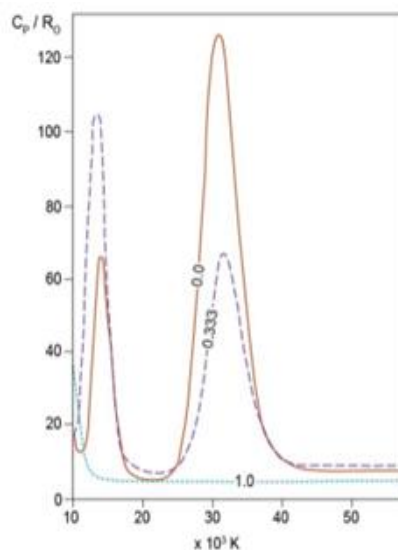


FIG.1 Plot of specific heat against temperature at $1-6 \cdot 10^4$ K for particle densities from 10^{10} to 10^{-6} g cm^{-3} and for hydrogen unit volumes of 0.333 and 1.0 equivalent to 50% and of 100% hydrogen by volume [11].

In our model of the Sun, induction is by way of electromagnetic energy derived from spinning convective pseudo-Taylor columns in the Rayleigh-Bénard setting of the convection zone - pseudo in the sense that they may develop in a fluid subject to strong rotation and thermal forcing although without the basal obstacle of the original definition [12-14]. Large-scale vortices are a possible outcome of rotating planar convection in an electrically conducting Boussinesq fluid [15]. The associated dynamos generate magnetic fields that are concentrated in the shear layers surrounding the vortices, although for Rayleigh numbers just above a critical value the convection takes the form of elongated columns with a small horizontal cross-section and is aligned with the rotation axis [16]. These are the structures that govern photospheric granulation [2].

The columnar model evidently differs from the classic notion of a primarily convective mechanism for granulation [17]. The summit of the columns is manifested as mesogranulation and supergranulation; the surface flow field is accordingly in close agreement with the magnetic field [18]. The columns are free to spin, even if closely packed because they are insulated mechanically by sheaths [19]. Indeed, Spacelab-2 white-light images illustrate both clockwise and anticlockwise spin; they also show that photospheric vorticities can twist a magnetic flux tube by 360° in < 3 hours, that is an average of $> 2^\circ/\text{min}$ [18]. Tangential (vertical) flows associated with the average supergranule outflow are indeed reported to reach about 10 m s^{-1} [20].

The fluid uppermost photosphere in which they spin is partly ionized and therefore electrically conducting. The cylindrical support is irrelevant except insofar as it creates quasi-regular spacing of planar rotating discs at the photospheric surface. Large-scale-vortex dynamos, which call for magnetic Reynolds numbers ~ 100 to 550 , are here proposed as the source of basal chromospheric heating [21,22]. An analogy with the H/He atmospheric evolution of young terrestrial planets points to XUV radiation as a plausible supplementary heating source [23]; XUV emission by the upper chromosphere and the TR was demonstrated by a slit spectrograph observation from Skylab [24].

Magnetic energy flux at the photosphere has been evaluated at active regions, such as NOAA 11158, by modelling complemented by Hinode satellite observations [25]. At one plage region the vertical Poynting flux had values of about $5 \pm 1 \times 10^7 \text{ erg cm}^{-1}\text{s}^{-1}$, close to the energy loss ($\sim 2 \times 10^7 \text{ erg cm}^{-2}\text{s}^{-1}$) estimated for active-region fields in the chromosphere [26,27]. The dominant heating mechanism, one of three discussed by Goodman, is resistive dissipation of the proton (Pedersen) currents driven by the convection electric field that we have visualized as spinning columns [28].

Indeed, the modelling by Goodman leads to the proposition consistent with the theme of this paper that the chromosphere of the Sun (away from flaring regions) is *created* by Pedersen current dissipation [29]. Heating by Pedersen current dissipation is very inefficient when the plasma is fully ionized and strongly magnetized, somewhat above $\sim 2170 \text{ km}$, consistent with the value of 2500 km for the lower boundary of the Transition Region cited earlier [30,6].

Step II

In a preliminary version of the tripartite scheme, the Joule-Thomson (J-T) effect was put forward as the pertinent heating system for the transition region though without the throttling that was included in the classic experiments by Thomson & Joule (1853) [2,31]. In the absence of experimental data for the temperatures at issue the term J-T is provisionally retained for the heating of a H/He plasma which is associated with a reduction in electron density n_e from $\sim 10^{19}$ to 10^{15} m^{-3} , that is to say when a strong negative density gradient in the quiet Sun coincides with a strong positive temperature gradient [32].

In a widely reproduced diagram, the onset of the TR corresponds to a plasma particle density N (as distinct from 'plasma density')

commonly used to signify electron density) of slightly more than 10^{16} m^{-3} **FIG. 2** [33]. Photoionization of hydrogen reduces its cooling efficiency by some six orders of magnitude so that at high temperatures (10^4 - 10^8 K) neutral hydrogen cools at about $10^{-18} \text{ erg cm}^3\text{s}^{-1}$ compared to $2.10^{-24} \text{ erg cm}^3\text{s}^{-1}$ for ionized hydrogen, with a peak (to judge from the published data) at $\sim 10^3 \text{ K}$ [34]. Photoionization has a similar effect on helium, which when partially ionized cools very efficiently by blackbody radiation and direct coupling to the helium Lyman continuum [35]. Once fully ionized by further heating, however, it no longer couples well to the continuum (the Lyman limit being 91.2 nm, 13.6 eV). This signals the end of radiative loss or, in other words, the onset of uninhibited heating, and temperatures of 10^6 K are rapidly attained. In short, the trigger is more in the nature of a safety catch which is released at a critical temperature.

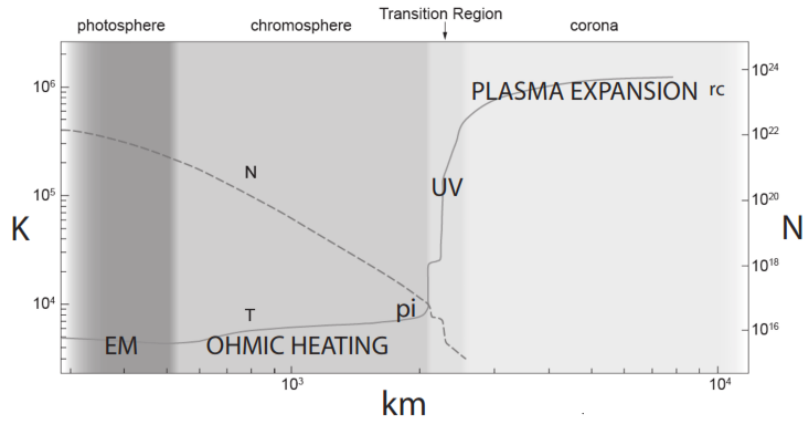


FIG. 2 Proposed heating episodes and the intervening triggers set against major subdivisions of the solar atmosphere and plots of temperature (T) and plasma particle density (N). EM = electromagnetic energy, pi = photoionisation, rc = radiative cooling; T and N after [33].

A value of $\sim 6.10^3 \text{ K}$ signals the region where cooling by radiation begins to nullify EUV heating as shown by radiative cooling functions for $^3\text{HeH}^+$ and $^4\text{HeH}^+$ **FIG 3** [36]. Here the rate of cooling attains between 10^{-10} to 10^{-9} erg/s . Indeed the calculated radiative cooling function (in $\text{erg cm}^{-3}\text{s}^{-1}$) at temperatures $> 10^4 \text{ K}$ for plasmas at low densities with solar abundances in collisional ionization equilibrium K drops rapidly from 10^5 to $10^{7.5} \text{ K}$ [37].

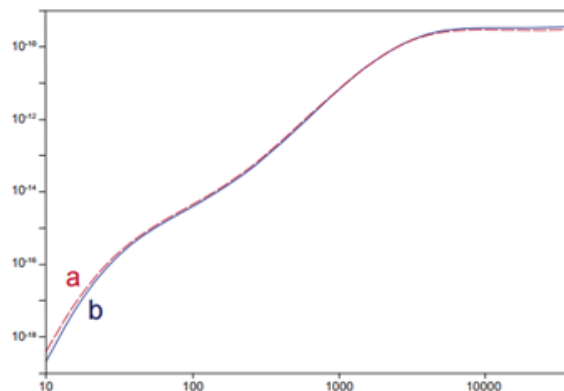


FIG. 3 Radiative cooling function (erg/s) of HeH plasma [36]. a = $^3\text{HeH}^+$, b = $^4\text{HeH}^+$

Step III

The upper limit of the TR may be defined as about 5.10^6 m above the photosphere by a deceleration in the temperature increase than in progress. Thereafter heating, triggered by propinquity to the near-vacuum of space, continues equably. Gurevich *et al.* and Gurevich & Pitaevsky were perhaps the first to show that the expansion of a plasma into a vacuum or a more tenuous plasma could result in the acceleration of ions to high energies, a process for which the self-similar solution indicates a logarithmic increase in velocity [38-41,23]. Plasma expansion has been investigated experimentally as well as theoretically even though the circumstances that concern us here, viz. temperatures of 10^6 K and coronal pressures of perhaps $1.3 \cdot 10^{-11}$ Pa, present even more serious laboratory limitations than does the ohmic heating of plasmas in the chromosphere [42,43]. But heating of He^{++} ions in the solar wind has long been recorded by spacecraft [44].

The bearing of this effect on space phenomena was made explicit by the interaction of an obstacle with a plasma. Relation between pressure fall and temperature in an astronomical context was assumed by Kothari when he showed that, for a relativistically degenerate gas (i.e. one nearing its ground state) undergoing Joule-Thomson expansion, the degree of heating per unit fall of pressure increased with the degree of degeneracy [45]. Samir & Wrenn reported that ionospheric electron temperature measured by a Langmuir probe in the near wake of an artificial satellite (Explorer 31) was raised above that of the ambient electron gas by as much as 50% [46]. They referred to earlier work on the Gemini/Agena spacecraft in which wake temperature was 1700 K greater than the ambient temperature in one experiment and 764 K in another [47]. The Moon's wake provided scope for related work; the increase in the electron temperature in the lunar wake found by the SWE plasma instrument on the WIND spacecraft amounted to a factor of four although ion temperatures were little changed [48]. Laboratory investigations based on immersion of a plate in a single-ion, collisionless, streaming plasma, saw 'early time expansion' result in ion acceleration into the wake [49].

Conclusion

Contrary to the accepted puzzling notion that the transition region and even the chromosphere are heated inwards from the corona, the temperature rise is cumulatively radial. What is more, structuring the solar atmosphere into three major zones is not the source of our stepwise heating sequence but its outcome.

The coherence between solar wind variations and sunspot activity **FIG. 4** is consistent with our proposed tripartite heating scheme: induction heating, which brings temperatures up to 20,000 K and triggers Joule-Thomson heating, which in turn results in temperatures of 250,000 K at the transition region, and thereafter plasma expansion into the near vacuum of space, which is here proposed as the mechanism by which temperatures of 1-2 million K are raised in the corona before it grades into interstellar space. The long-term record of the Sun's activity, essential for robust interpretation of paleoclimates as well as for assessing the solar factor in weather, requires detailed information on the source of EUV fluctuations. Measurements by the EVE instrument on the Solar Dynamics Observatory satellite combined with neutrino data suggest that the UV flux is modulated primarily by rotation of the solar interior (provisionally named the Dicke Cycle) rather than the passage of active areas across the solar disc. Thus periodicities recorded by cosmogenic isotopes such as ^{10}Be , which respond to oscillations in the strength of the solar wind, are better guides to the solar factor than observed sunspot records and have the advantage of spanning $> 10^5$ yr rather than a mere 4.10^2 yr. In short, solar wind emerges as the one dependable indicator of solar activity. Sunspot data are compromised by their indirect relation to the Sun's irradiance: the rotation of active areas reportedly explains no more than 42% of its variation.

The proposed scheme could help to explain heating in other bodies (such as Titan) which display a radial increase in temperature and a decrease in plasma density as well as sustained gas outflow. It may also bear on the thermal evolution of other coronal stars.

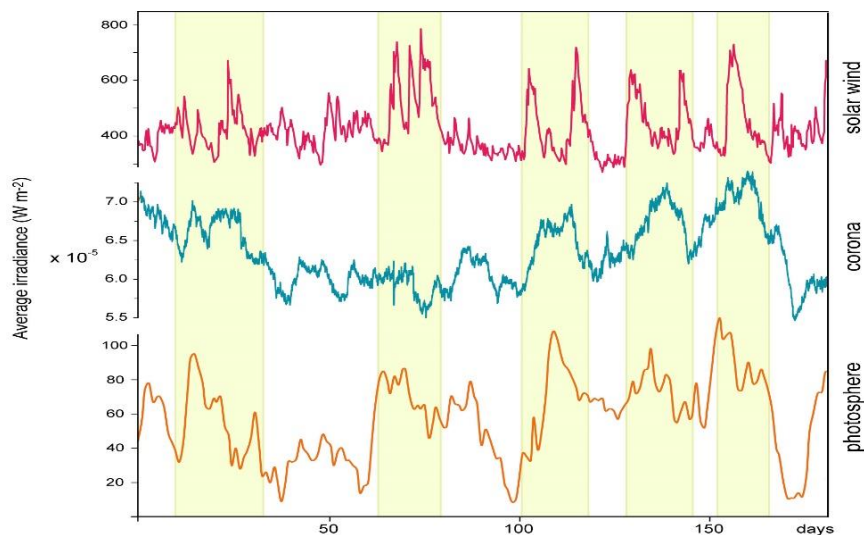


FIG. 4 Irradiance variation for 1 Jan-1 July 2012 for the photosphere, the solar corona, and the solar wind. Plots and scale details (W m^{-2}) in [2].

REFERENCES

1. Amari T, Luciani J-F, Aly J-J. Small-scale dynamo magnetism as the driver for heating the solar atmosphere. 2015;522(7555):188-91.
2. Vita-Finzi, C. The Sun Today. Springer, Cham. 2018;59-73.
3. Morse E. Nuclear Fusion. Springer, Cham. 2018;23-37.
4. Peter H, Marsch E. Hydrogen and helium in the solar chromosphere: a background model for fractionation. *Astron. Astrophys.* 1998 May;333:1069-81.
5. Behringer KH, Carolan PG, Denne B et al. Impurity and radiation studies during the JET ohmic heating phase. *Nuclear fusion.* 1986;26(6):751-86.
6. NASA. Sun fact sheet. nssdc.gsfc.nasa.gov. Retr Nov 2019.
7. Spitzer Jr L. The stellarator concept. *Phys. Fluids.* 1958 Jul;1(4):253-64.
8. O'Brien MR, Robinson DC. Tokamak experiments. In Dendy R (ed) *Plasma Physics: an Introductory Course*. Cambridge Univ Press, Cambridge. 1993;189-208
9. ESA 2013. Retrieved. 2019.
10. Judge PG, Peter H. The structure of the chromosphere. *Solar composition and its evolution-from core to corona.* 1998:187-202.
11. MS Nelson HF. Thermodynamic properties of hydrogen-helium plasmas. NASA, 1971
12. Taylor GI. Experiments with rotating fluids. *Proc. R. Soc. Lond. Series A.* 1921 Nov 1;100(703):114-21.
13. Grooms I, Julien K, Weiss JB, et al. Model of convective Taylor columns in rotating Rayleigh-Bénard convection. *Phys Rev Lett.* 2010;104(22):224501.
14. King EM, Aurnou JM. Thermal evidence for Taylor columns in turbulent rotating Rayleigh-Bénard convection. *Phys Rev E.* 2012;85(1):016313.
15. Guervilly C, Hughes DW, Jones CA. Large-scale vortices in rapidly rotating Rayleigh-Bénard convection. *J Fluid Mech.* 2014;758: 407-35.
16. Guervilly C, Hughes DW, Jones CA. Generation of magnetic fields by large-scale vortices in rotating convection. *Phys Rev E.* 2015;91(4):041001.
17. November LJ. Inferring the depth extent of the horizontal supergranular flow. *Sol. Phys.* 1994 Sep;154(1):1-7.
18. Simon GW et al Relation between photospheric flow fields and the magnetic field distribution on the solar surface. *Astrophys J* 1988; 327.

19. Sprague M, Julien K, Knobloch E, et al. Numerical simulation of an asymptotically reduced system for rotationally constrained convection. *J. Fluid Mech.* 2006 Mar;551:141-74.
20. Langfellner J, Gizon L, Birch AC. Spatially resolved vertical vorticity in solar supergranulation using helioseismology and local correlation tracking. *Astron Astrophys.* 2015; 581:67.
21. Guervilly C, Hughes DW, Jones CA. Large scale vortex dynamos in planar rotating convection. *J Fluid Mech.* 2017;815: 333-60.
22. Bushby PJ, Käpylä PJ, Masada Y, et al. Large-scale dynamos in rapidly rotating plane layer convection. *Astro Astrophys.* 2018;612: A97.
23. Erkaev NV, Lammer H, Odert P, et al. XUV-exposed, non-hydrostatic hydrogen-rich upper atmospheres of terrestrial planets. Part I: Atmospheric expansion and thermal escape. *Astrobiology.* 2013;13(11): 1011-29.
24. Doschek GA, Feldman U, Tousey R. Limb-brightening curves of XUV transition zone lines in the quiet Sun and in a polar coronal hole observed from Skylab. *Astrophys. J.* 1975; 202:151-4.
25. Kazachenko MD, Fisher GH, Welsch BT et al. Photospheric electric fields and energy fluxes in the eruptive active region NOAA 11158. *Astrophys J.* 2015;811(1):16.
26. Welsch BT. The photospheric Poynting flux and coronal heating. *Publ. Astron. Soc. Jpn.* 2015 Apr 1;67(2):18.
27. Withbroe GL, Noyes RW. Mass and energy flow in the solar chromosphere and corona. *Annu Rev Astron Astrophys.* 1977;15:363-387
28. Goodman ML. On the mechanism of chromospheric network heating and the condition for its onset in the Sun and other solar-type stars. *Astrophys J.* 2000;533(1):501.
29. Goodman ML. On the creation of the chromospheres of solar type stars. *Astron Astrophys.* 2004a;424(2):691-712.
30. Goodman ML. On the efficiency of plasma heating by Pedersen current dissipation from the photosphere to the lower corona. *Astron Astrophys.* 2004;416(3):1159-78.
31. Thomson W, Joule JP (1853) On the thermal effects of fluids in motion. *Phil Trans Roy Soc London* 143: 357–365
32. Lemaire P. Structure and role of the transition region. In 8th SOHO Workshop: Plasma Dynamics and Diagnostics in the Solar Transition Region and Corona. 1999;446: 35-42.
33. Peter H. Structure and dynamics of the lower corona of the Sun. *Rev Mod Astron.* 2004;17: 87-
34. Gnat O, Ferland GJ. Ion-by-ion cooling efficiencies. *Astrophys J Suppl Ser.* 2012;199(1):20.
35. Oppenheimer BD, Schaye J. AGN proximity zone fossils and the delayed recombination of metal lines. *Mon. Not. R. Astron. Soc.* 2013 Sep 11;434(2):1063-78.
36. Coppola CM, Lodi L, Tennyson J. Radiative cooling functions for primordial molecules. *Mon Not R Astron Soc.* 2011;415(1):487-93.
37. Draine BT (2011) *Physics of the interstellar and intergalactic medium.* Princeton Univ Press, Princeton NJ
38. Gurevich AV, Pariiskaya LV, Pitaevskii LP. Self-similar motion of rarefied plasma. *Sov Phys JETP.* 1966;22(2):449-54.
39. Gurevich AV, Pitaevskii LP. Non-linear dynamics of a rarified ionized gas. *Prog Aerosp Sci.* 1975; 16:227-272.
40. Samir UR, Wright Jr KH, Stone NH. The expansion of a plasma into a vacuum: Basic phenomena and processes and applications to space plasma physics. *Rev. Geophys.* 1983 Aug;21(7):1631-46.
41. Crow JE, Auer PL, Allen JE. The expansion of a plasma into a vacuum. *J. Plasma Phys.* 1975 Aug;14(1):65-76.
42. Chan C. Laboratory experiments on plasma expansion. *Ion Accel. Magnetos. Ionos.* 1986 Jan 1;38:249-53.
43. Elkamash IS, Kourakis I. Multispecies plasma expansion into a vacuum: The role of secondary ions and suprathermal electrons. *Phys. Rev. E.* 2016 Nov 7;94(5):053202.
44. Ofman L, Viñas AF, Maneva Y. Two-dimensional hybrid models of H+He++ expanding solar wind plasma heating. *J. Geophys. Res.: Space Phys.* 2014 Jun;119(6):4223-38.
45. Kothari DS. The theory of pressure-ionisation and its applications. *Proc Roy Soc London A.* 1938; 165:486-500.
46. Samir U, Wrenn GL. Experimental evidence of an electron temperature enhancement in the wake of an ionospheric satellite. *Planetary and Space Science.* 1972 Jun 1;20(6):899-904.
47. Medved DB. Measurement of ion wakes and body effects with the Gemini/Agema satellite. casi.ustr.gov.19700042169
48. Ogilvie KW, Steinberg JT, Fitzenreiter RJ, et al. Observations of the lunar plasma wake from the WIND spacecraft on December 27, 1994. *Geophys. Res. Lett.* 1996 May 15;23(10):1255-8.
49. Wright KH, Stone NH, and Samir U. A study of plasma expansion phenomena in laboratory generated plasma wakes: Preliminary results. *J. plasma phys.* 1985 Feb;33(1):71-82.